KeAi CHINESE ROOTS GLOBAL IMPACT
International Journal of Innovation Studies

OPTIMIZED URBAN DRAINAGE NETWORK DESIGN USING GRAPH THEORY AND ARCHIMEDES INSPIRED SEARCH AND RESCUE ALGORITHM

J. Suganthi[1], I. Paulraj Jayasimman[2]
[1]Research scholar of Maritime Education and Training (AMET), Deemed to be University, India Email: sugisuresh27@yahoo.in
[2]Associate Professor, Department of Mathematics, Academy of Maritime Education and Training (AMET), Deemed to be University, India.
Corresponding Author mail ID - ipjaysimman@ametuniv.ac.in

Abstract

Urban drainage systems play a critical role in managing storm water and mitigating flooding in rapidly growing cities. Designing efficient and resilient drainage networks remains a significant challenge due to complex urban topologies, variable rainfall patterns, and increasing surface runoff. Existing design approaches often fall short in optimizing network layouts for cost-effectiveness, flow efficiency, and adaptability to environmental stressors. To address these challenges, this research proposes an optimized urban drainage network design framework that integrates Graph Theory with the Archimedes-Inspired Search and Rescue Optimization (AISRO) Algorithm. Graph Theory is employed to model the urban layout as a network of nodes and edges, enabling the analysis of connectivity, flow paths, and critical junctions. The Archimedes Optimization Algorithm, inspired by buoyancy and equilibrium principles, is adapted for search and rescue optimization to enhance the placement and sizing of drainage components for optimal performance. The main objective of the study is to improve the hydraulic efficiency, cost-effectiveness, and resilience of urban drainage networks. Experimental simulations conducted on benchmark urban layouts demonstrate that the proposed hybrid approach outperforms existing methods in terms of reduced flooding incidents, optimized pipe sizing, and lower construction costs. The results validate the potential of the combined approach to support smart and sustainable urban infrastructure planning.

Keywords: Urban Drainage Network; Graph Theory; Archimedes Optimization Algorithm; Search and Rescue Optimization; Network Design; Hydraulic Efficiency; Flood Mitigation; Smart Infrastructure; Sustainable Urban Planning; Metaheuristic Optimization

1. Introduction

Over the past two decades, there has been a significant increase in processing power, which has enabled access to vast amounts of information across biological, technical, social, and financial systems. This growing understanding has contributed to making our daily lives safer and more efficient. In the 1960s, random graph theory the earliest network modelling framework was introduced. Given the rapid evolution of real-world networks and the development of more advanced graph-based technologies, random graph theory is no longer sufficient for accurately representing modern networks [1]. A fundamental field of research in computer science and mathematics, graph theory examines graphs are fundamental mathematical frameworks designed to capture pairwise interactions between entities. These graphs function as maps showing the relationships between different elements, as they are made up of nodes and connecting edges. Edges in this paradigm can be directed indicating directed or undirected emphasizing equivalence between connected nodes [2]. Due to their adaptability, graphs are essential tools in discrete mathematics enabling the representation and analysis of complex structures. This is especially relevant when modelling transportation networks. Graphs are frequently used to depict Software-Defined Networking (SDN) in communications [3]. Undirected graphs are commonly employed to depict urban water distribution systems, which are characterized by bidirectional flows. Directed graphs are used to illustrate wastewater networks, where the flow is unidirectional towards the Wastewater Treatment Plant (WWTP). In densely populated areas, urban water networks are essential supporting the critical processes required to maintain urban life [4]. These vital infrastructures responsible for the supply, distribution, and management of waste water ensure access to clean water for consumption, hygiene, and commercial purposes. Often operating in the background, these systems are sometimes overlooked amid the bustling activity of metropolitan areas. In our rapidly evolving technological era, computer science provides advanced solutions commonly applied in high-tech domains such as communication networks often underutilized in other scientific fields [5]. The importance of urban water networks cannot be overstated. It serve as the backbone of urban infrastructure, facilitating the functioning of homes, businesses, hospitals, and industries. Two urgent issues in water science that demand attention are the need for wastewater surveillance for SARS-CoV-2 detection and the optimization of resilient reclaimed water networks to tackle the severe problem of water scarcity especially in Mediterranean regions [6]. The application of computer science solutions to these challenges could offer valuable insights and innovative approaches for the advancement of urban water networks. Without reliable access to drinking water, cities would come to a standstill, with severe repercussions for economic activity, healthcare systems, and overall quality of life. The efficient, robust, and dependable functioning of urban water systems significantly impacts both daily living and national economic development [7].

Due to increasing impermeable surfaces, extreme weather events, and intensified human activity, Urban Water Networks (UWNs**)** are under serious threat from climate change, population growth, and global urbanization. UWM processes including planning and design, implementation, and maintenance of associated water systems are essential to meet the growing demands for drinking water supply, sanitation, infiltration, and storm water runoff mitigation [8]. Water infrastructure including water reuse systems must be comprehensively reimagined to promote circularity and reduce the consumption of potable water. A significant volume of clean water can be conserved by utilizing treated wastewater for various non-potable purposes such as industrial operations, vehicle washing, toilet flushing, household cleaning and supplementary water supply [9]. In light of increasing climatic unpredictability and severe storm events, resilience is a critical attribute for UWNs. These networks must maintain service delivery despite numerous challenges, including droughts that affect Water Distribution Networks (WDNs) and tree root intrusions that impair wastewater systems [10]. Wastewater networks are particularly vulnerable to numerous hazards often resulting in leaks that compromise public health and incur substantial economic losses. Beyond the direct costs of repairs, pipe failures lead to collateral expenses such as structural damage, business interruptions, and production losses [11].

Public health issues, disruption of essential services, substantial financial burdens, and the waste of significant water resources are among the serious consequences of failures in urban water systems. Automated resilient design alternatives offer a practical solution to prevent network breakdowns in both potable and recycled WDNs by providing cost-effective and hydraulically tested strategies, thereby conserving substantial amounts of water over time [12]. External factors such as population growth, urbanization, aging infrastructure, and global warming pose financial and public health risks to urban water infrastructures, particularly Urban Drainage Networks (UDNs**)**. UDNs must be equipped to handle both typical and extreme load scenarios [13]. While most existing research has focused on enhancing the resiliency of sewage network rehabilitation such as through critical link analysis the influence of a system's topological design during the planning phase has been largely neglected. There have been relatively few efforts to explore decentralization in UDNs, particularly regarding topological architecture [14].

For example, spanning tree technique to study hybrid design configurations for waste water treatment facilities. Methodology could not be adapted for the development of optimal storm water networks due to the specific objectives and constraints selected. These limitations make the approach less applicable to real-world scenarios in flat terrains or partially developed UDNs [15]. Although their decentralized strategy yielded promising results in a flat-region case study, several limitations hindered practical application on a larger scale. For instance, their model focused solely on minimizing construction costs for distributed networks, requiring numerous hydraulic calculations to approximate optimal outcomes [16]. UWM remains a complex challenge due to the multitude of design options, competing objectives, and uncertainty arising from rapidly changing environmental and urban conditions. In recent years, the interdisciplinary application of network science has garnered growing attention from researchers as a means of addressing these complexities [17].

To address these limitations, complex network theory emerged and has since made substantial progress in understanding the structure and function of intricate networks. WDNs and UDNs are two critical components of urban water infrastructure that have significantly benefited from the application of complex network analysis in both their design and maintenance [18]. In recent years, several high-impact academic journals have published research proposing various techniques and metrics aimed at improving our ability to characterize, understand, and optimize the topology of UWNs [19]. To address these vulnerabilities, the concept of urban water security has emerged, facilitating comprehensive risk management strategies and fostering a deeper understanding of the intricate interactions between human and environmental systems. This computational approach supports the evaluation of whether it is more effective to repair leaks and failures as they occur or to proactively mitigate risks by relocating nearby hazards. Resiliency in WDNs is particularly critical, as pipe failures have extensive environmental and economic repercussions that extend well beyond the immediate disruption [20].

2. Related Works

In contemporary and smart cities, the efficient operation of water supply and UDNs is vital. UDNs can take the form of either combined systems also manage storm water runoff during rain events, or sanitary systems collect and transport only wastewater. Their design and performance are primarily influenced by geographical features (such as slope) and their connectivity typically follows the layout of the urban road network. These systems consist of numerous interconnected components [21]. In recent years, the need to propose novel management and analytical methods for such critical infrastructure has become increasingly in response to the impacts of unchecked urbanization, aging infrastructure, and accelerating climate change. To address the challenge of UDN rehabilitation under uncertainty, proposed two optimization approaches within a unified framework that incorporates multiple economic and performance-based objectives [22]. The first approach accounts for uncertainties in the objective function evaluation, while the second addresses uncertainties within the optimization process itself. Despite their differences, both methods yield nearly identical results and identify solutions that are reliably optimal in terms of both cost and potential damage mitigation. A comparative analysis of multifaceted adaptive algorithms for the hydraulic rehabilitation of urban sewer systems has also been introduced, showing promise in terms of feasibility and cost-effectiveness [23].

To anticipate future climate challenges, proposed the Adaptation Tipping Points (ATP) strategy to explore how changes in precipitation could affect UDN. A series of adaptation pathways introduced such as enhanced system storage and nature-based solutions linked to an economic analysis that incorporates long-term institutional planning and ecosystem services proposed. UDN rehabilitation strategy that includes installing storm water retention tanks and replacing outdated pipelines to address environmental and climatic changes [24]. In this context, resilience is a crucial concept that integrates the system's performance under typical loading conditions with its ability to minimize failures during atypical events. It provides a valuable metric for system management by capturing the capacity to reduce impacts from unexpected disruptions and anticipated changes such as global warming and increasing urbanization [25].

To identify critical components resulting from system malfunctions and to prioritize inspection and recovery efforts, proposed a preventive strategy for assessing drain risk. Utilized historical data while incorporating a range of physical, environmental, and operational factors influencing performance [26]. System monitoring in terms of hydraulic performance and effluent quality is another critical area of focus. All of the aforementioned methods require vast amounts of data and complex mathematical modelling to define hydraulic model parameters and reproduce dynamic behaviors [27]. Simulating the hydraulic characteristics of UDNs is often infeasible due to the systems' complexity, limited understanding of their full structure, or the unavailability of necessary data such as flow rates, pipe diameters, or the high cost of detailed topological surveys. Tools derived from Complex Network Theory (CNT) offer a promising alternative for analysing and managing such infrastructure. CNT is particularly well-suited for identifying key components nodes or links within a system, and for evaluating resilience and failure propagation [28].

The scalability and flexibility of graph-based methods make them particularly well-suited for decentralized storm water systems and expanding urban developments. To improve drainage system optimization, researchers are increasingly exploring advanced and bio-inspired algorithms. These include metaheuristic techniques such as the Archimedes-Inspired Search and Rescue Algorithm (AISRA) and hybrid models that integrate graph theory with Artificial Intelligence (AI). By mimicking physical laws, these methods can navigate complex design landscapes, avoid local optima, and accelerate convergence offering robust solutions for intelligent, resilient, and adaptive urban drainage planning when coupled with hydraulic models and GIS data. Well-designed urban drainage networks are essential for sustainable urban growth and climate resilience. Enable efficient storm water management, reduce flood risks, and lower infrastructure costs.

3. Problem Formulation

Under certain geographical and hydraulic restrictions, the objective is to enhance hydraulic performance while minimizing overall cost by optimizing the architecture and design variables of an urban water supply system. The optimized UDN design problem seeks to develop a cost-effective and hydraulically efficient drainage system by applying principles of graph theory and the Archimedes-Inspired Search and Rescue Algorithm (AISRA). The objective is to minimize the total cost C total includes pipe Installation, excavation, and maintenance costs. This is mathematically represented as:

$$\min C_{total} = \sum_{x=1}^{n}\left(C_{pipe_x} + C_{excavation_x} + C_{maintenance_x}\right) \quad (1)$$

To ensure the system is hydraulically sound, the flow through each pipe must satisfy Manning's equation: $Q_x = \frac{1}{n_m} A_x R_x^{2/3} S_x^{1/2}$ (2)

Where Q_x the discharge, n_m is the Manning's coefficient, A_x the flow area, $R_x$the hydraulic radius, and S_x the slope. At each junction node y, continuity constraints ensure that incoming and outgoing flows are balanced: $\sum Q_{in_y} = \sum Q_{out_y}$ (3)

The system layout is modelled as a graph $G = (V, E)$ where nodes V represent junctions or inlets and edges E represent pipes. The aim is to identify a minimum spanning subgraph that minimizes edge weights (costs) while maintaining connectivity:

$$\min \sum_{(u,v)\in E''} w(u,v) \; s.t. \; E' \subseteq E \quad (4)$$

AISRA is employed to solve the multi-constraint nonlinear optimization problem. The solution vector I_t iteration & is updated using: $I_{t+1} = I_t + \alpha.\left(F_{best} - F(I_t)\right) + \beta.r$ (5)

Where, α is the leaming rate, β controls exploration, and r adds stochastic diversity. The final salution must adhere to design constraints such as minimum pipe cover, feasible slopes, and velocity bounds. This hybrid approach ensures an efficient and sustainable urban drainage network design.

4. Materials and Methods

A hybrid methodological approach integrating network optimization, bio-inspired computing, and mathematical modelling is employed in the enhanced UDN design process using graph theory and the AISRA shown in Figure 1. This process utilizes various data sources, including city topology, geographical databases, rainfall data, pipe characteristics, and hydraulic constraints. The urban area is abstracted into a mathematical model, where potential pipe connections are represented as edges, and intersections, power sources, and inlets serve as nodes. Each edge is assigned a weight based on factors such as cost, slope, and hydrological feasibility. The process begins with pre-processing, during which GIS tools are used to extract flow direction and elevation data. A directed graph is then constructed, and potential optimal layouts are identified using graph theory principles such as the Minimum Spanning Tree (MST) and shortest path algorithms.

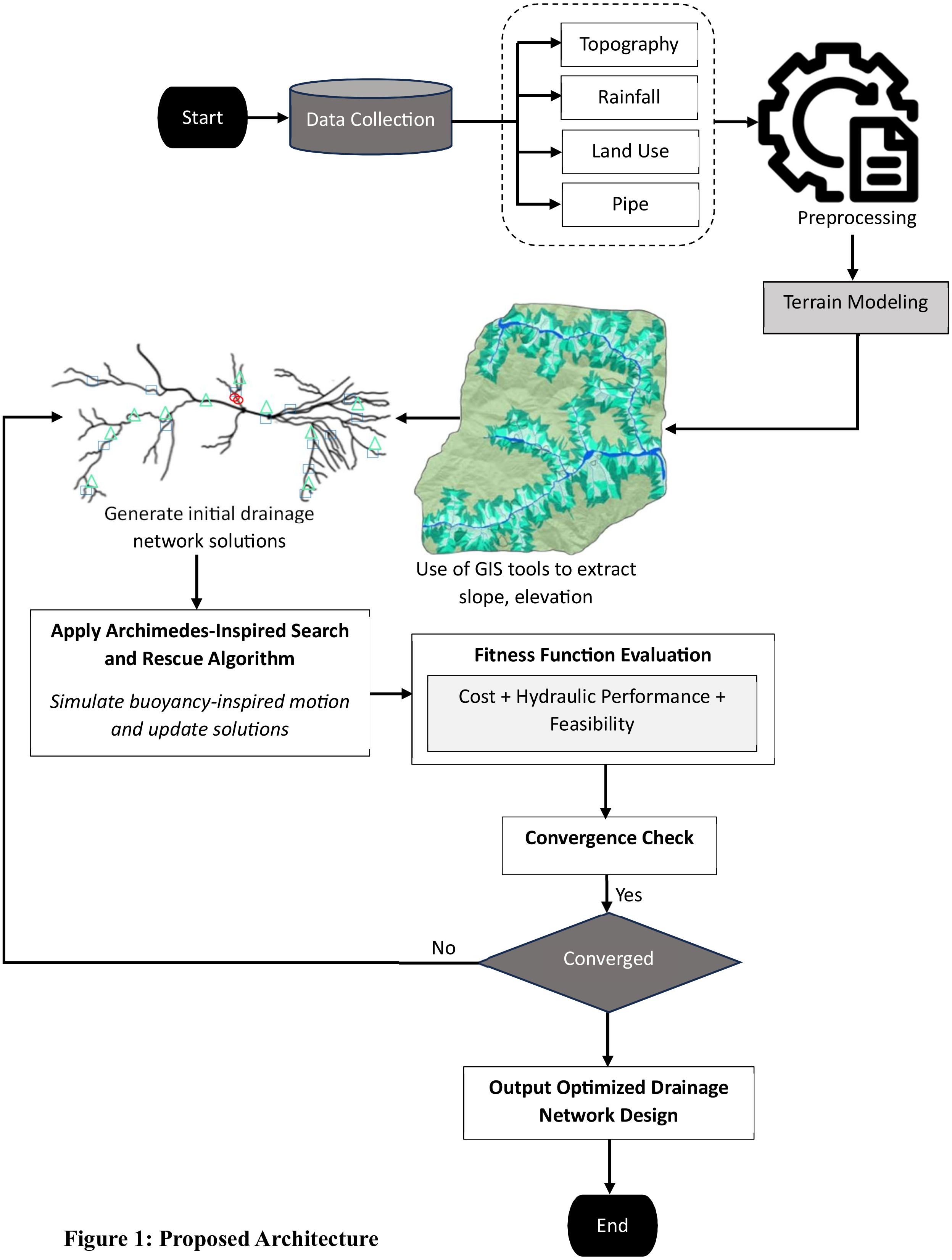

Figure 1: Proposed Architecture

A composite fitness function is formulated, incorporating both cost and hydraulic performance indicators while accounting for complex constraints like slope, discharge capacity, and minimum cover depth. This multi-objective optimization problem is addressed using the AISRA method inspired by search-and-rescue dynamics and Archimedes' principle of buoyancy. Through adaptive exploration and exploitation of the search space, the algorithm iteratively refines an initial set of drainage configurations. Each candidate solution is evaluated using the fitness function, which considers network feasibility, cost-efficiency, and hydraulic performance. The outcome is an optimized drainage layout that effectively balances hydraulic efficiency, environmental sustainability, and economic feasibility demonstrating the power of integrating computational optimization techniques with discrete network modelling.

4.1 Layout Generation of the Optimized Network

The layout generating procedure in an undirected network made up of edges and nodes where connections are regarded as pipes and nodes as manholes is guided by a graph-theoretic method in the present research. Based on the street topological structure, the first undirected base network is a full-mesh network that includes every possible arrangement. This procedure is depicted in Figure 2.

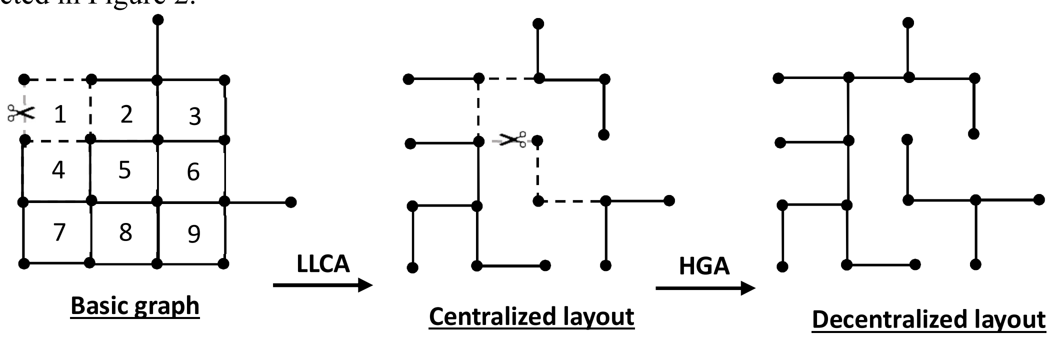

A fully looped diagram incorporating the entirety of feasible layout configurations

A tree layout with only one root node

In a completely decentralized layout, each substructure possesses exactly one root node

Figure 2: Layout generation process

The Loop-By-Loop Cutting Algorithm (LLCA) is initially employed to analyse the underlying graph by removing any cyclic paths. This ring-opening process is carried out iteratively until the base graph is transformed into a minimal spanning tree, with the output node designated as the root. The resulting tree such as fully centralized layout with a single outlet serves as the input for the decentralized layout generation procedure. To further partition the structured layout, the Hanging Garden Algorithm (HGA) is applied by specifying a predefined number of candidate outlets. It progressively opens the shortest paths between the newly defined drainage outlets and the existing outlet nodes in the current configuration. This process generates subsystems with multiple outflow points, resulting in layout patterns that exhibit varying degrees of decentralization. As the layout transitions from a single spanning tree to a forest of drainage systems composed of multiple spanning trees, a decentralized pattern is effectively formed. In the optimized UDN design using graph theory and AISRA, the urban drainage system is represented mathematically as a directed graph $G = (V, E)$ where V denotes the set of nodes (e.g, junctions, inlets) and E represents the set of edges (e.g. pipelines). Each edge carries a flow Q_{xy} calculated by $Q_{xy} = A_{xy}.v_{xy}$, where A_{xy} the pipe's cross-sectional area and

v_{xy} the velocity of the fluid through the pipe. The continuity equation $\sum Q_{in} = \sum Q_{out}$ ensures mass conservation at each junction by equating the total inflow and outflow.
The optimization process applies the AISRA imitates buoyancy and strategic search behavior. The agent's position is updated using:
$I_x(t+1) = I_x(t) + B_x.\left(I_b(t) - I_x(t)\right) + r.(I_r - I_x) \quad (6)$
Where, $I_x(t)$ is the current position of agent x, I_b the best-known solution, I_x is a random candidate solution, B_x a buoyant factor, and r is a random scalar that enhances exploration.
The fitness of each solution is evaluated using the function $F = w_1.C + w_2.H + w_3.P$ combining construction cost C, hydraulic performance H, and constraint penalties P with respective weights w_1, w_2, w_3 The construction cost is computed as $C = \sum L_{xy}.c_{xy}$ where L_{xy} the pipe length and c_{xy} is the unit cost. These equations guide the algorithm toward optimal, cost-effective, and hydraulically sound drainage designs.
Urban Drainage Network (UDN) as a Graph: A UDN is modeled as a directed graph $G = (V, E)$ where V is the set of nodes (manholes, junctions, inlets); E is the set of edges (pipe segments).
Flow Rate in a Pipe: The volumetric flow Q_{xy} between node x and node y is given by
$Q_{xy} = A_{xy}v_{xy} \quad (7)$
Where A_{xy} is the cross-sectional area of the pipe and v_{xy} the flow velocity.
Continuity (Mass Conservation) at a Junction: For every node k in the network, the sum of inflows equals the sum of outflows: $\sum_{x:(x\to k)} Q_{xy} = \sum_{y:(k\to y)} Q_{ky} \quad (8)$
Manning's Equation for Hydraulic Capacity
Each pipe must satisfy: $Q_x = \frac{1}{n_m} A_x R_x^{2/3} S_x^{1/2} \quad (9)$
with n_m = Manning's roughness, A_x = flow area, R_x = hydraulic radius, and S_x = s slope.
Construction Cost Function: The total cost C of the network is
$C = \sum_{(x,y)\in E}\left(c_{xy}L_{xy}\right) \quad (10)$
Where c_{xy} is the unit cost per length and L_{xy} is the length of pipe (x, y)
Multi-Objective Fitness Function: Candidate designs are evaluated by
$F = w_1C + w_2H + w_3P \quad (11)$
Where, C = total cost, H = performance metric, P = penalty for constraint violations,w_1,w_2, w_3 = weighting factors.
AISRA Position Update Rule: The AISRA updates each solution X (t) by
$I_x(t+1) = I_x(t) + B_x(I_b(t) - I_x(t)) + r(I_r - I_x(t)) \quad (12)$
Where I_b is the best solution so far, I_r is a random solution, B_x is a buoyancy factor, and r is a random scalar.
4.2 Dataset description
In Metropolis X (12.9716° N, 77.5946° E), a 150 km² urban watershed defined by city GIS shape files, the investigation was carried out. A 30m resolution Digital Elevation Model (DEM) obtained from SRTM and local surveys was used to assess the terrain topography shown in Table 1. The National Meteorological Administration provided the historical hourly rainfall records (2025–2025) as a series of CSV files. While the Water Utility Authority supplied the previous pipe system in GIS format, containing dimensions, angles, and substances, land utilization and land cover data were obtained from Sentinel 2 images at a resolution of 10m.

The National Soil Survey provided the soil type maps and rates of infiltration (50m raster). To support hydraulic efficiency simulation, Manning's roughness estimates for different pipe materials were gathered from literature and field studies and arranged in tabulated CSV form.

Table 1: Dataset Description

Category	Parameter	Description	Source	Format / Resolution
Study Area	Location	Metropolis X (12.9716° N, 77.5946° E)	Municipal GIS Department	Vector shapefile
Study Area	Catchment Area	Urban catchment covering 150 km²	City Planning Office	Polygon shapefile
Input Data	Elevation	Digital Elevation Model of Terrain	SRTM / City Survey	Raster (30 m)
Input Data	Rainfall	Historical hourly rainfall (2010–2020)	National Meteorological Department	Time series CSV
Input Data	Land Use	Land-use/land-cover classification	Sentinel-2 satellite imagery	Raster (10 m)
Input Data	Pipe Network	Existing pipelines with diameter, slope, material	Water Utility Authority	GIS shapefile
Input Data	Soil Properties	Soil type and infiltration rates	National Soil Survey	Raster (50 m)

Table 2: Sample Data

Node ID	Latitude	Longitude	Elevation (m)	Land Use	Rainfall Intensity (mm/hr)	Pipe Diameter (mm)	Slope (%)	Manning's n	Soil Infiltration (mm/hr)
N1	12.9715	77.5948	915	Residential	20	300	0.8	0.013	8
N2	12.9730	77.5952	920	Commercial	25	450	1.0	0.014	5
N3	12.9742	77.5939	905	Industrial	30	600	0.5	0.015	3
N4	12.9760	77.5965	930	Green Space	15	300	0.7	0.013	12
N5	12.9781	77.5927	910	Mixed Use	18	450	0.9	0.014	7

Key characteristics for five typical drainage nodes (N1–N5) in the research region are compiled in the original database. Each record includes altitude and geographical coordinates (latitude and longitude) together determine the topographical location of the nodes. Local percolation capacity is represented by the "Soil Infiltration" rate. Table 2 includes the geographical, meteorological, and hydraulic factors necessary for optimal modelling of drainage networks.

4.3 Drainage network analysis using graph theory

In graph-theoretic modelling, the urban drainage network is represented as a directed graph $G = (V, E)$ where each junction or manhole is a node $v \in V$ and each pipe segment is a weighted edge $(x, y) \in E$ with weight w_{xy} reflecting construction cost or hydraulic resistance. Connectivity is encoded by the adjacency matrix A (where $A_{xy} = 1$ if $(x, y) \in E$ otherwise) and the degree matrix D (with $D_{xy} = \sum_y A_{xy}$), yielding the Laplacian $L = D - A$, whose properties inform network resilience. Flow conservation at node k is enforced by Equation (8) Hydraulic capacity on each edge follows Manning's law using Equation (9). Ensuring feasibility of flow rates. The optimization seeks a spanning subgraph $G' = (V, E') \subseteq G$ minimizing total weight $\min_{E' \subseteq E} \sum_{(x,y)\in E'} w_{xy}\ s.t.\ G'\ is\ connected,$ often solved through minimum spanning tree algorithms combined with metaheuristic refinements hydraulic and topographic constraints.

A WDN such as the one illustrated in Figure 3, consists of a series of interconnected pipes, each characterized by specific length, diameter, and friction resistance coefficients. The network variou[...]ponents within each conduit such as pumps, connectors, and valves. Pumps are in[...] junction nodes to maintain adequate pressure and meet consumer demand.

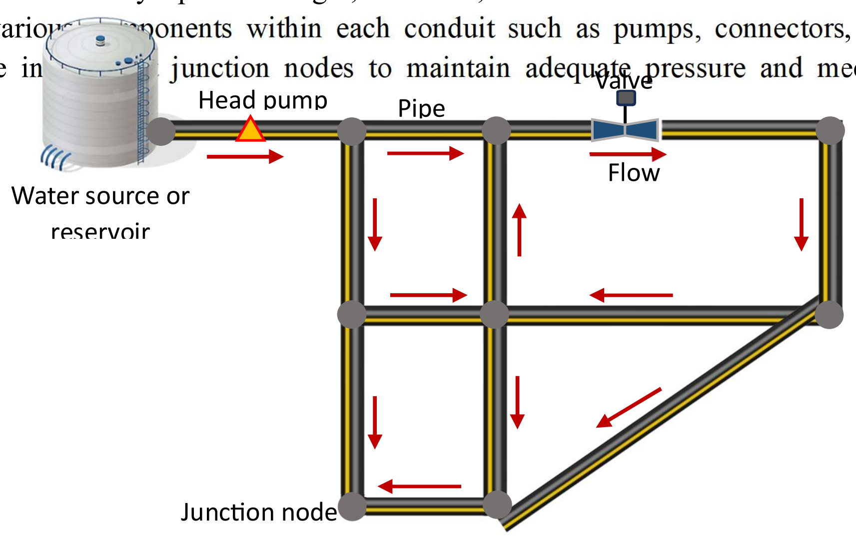

Figure 3: WDN representation

To address potential adverse conditions, a steady-state hydraulic model provides a comprehensive understanding of the pipe system and its components insights into system state estimation. Dynamic hydraulic systems utilize real-time sensor data collected from elements like water consumption meters continuously evaluate the system's current status and autonomously generate control signals for various network components. This real-time approach can significantly enhance the efficiency of the WDN.

4.4 Terrain-based direction control unit

Some flow directions must be adjusted, resulting in unfavourable gradients known as negative slopes lead to increased excavation volumes. This approach is particularly useful in steep and uneven terrain. In practice, pipes may still need to be installed against the natural ground slope, even though the region's steep landscape reveals general patterns for monitoring, routing, and installing gravity pipelines. Certain directions must be modified to point toward a feasible outlet.

(a) Initiating the process with a directed base graph where flow directions are based on natural ground elevations

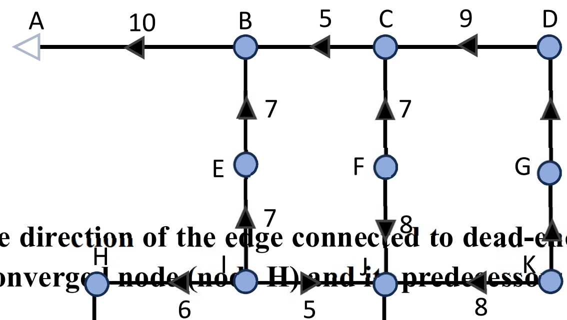

(b) Adjusting reversing the direction of the edge connected to dead-end node (edge ML) and then identifying the converged node (node H) and its predecessors (nodes and M)

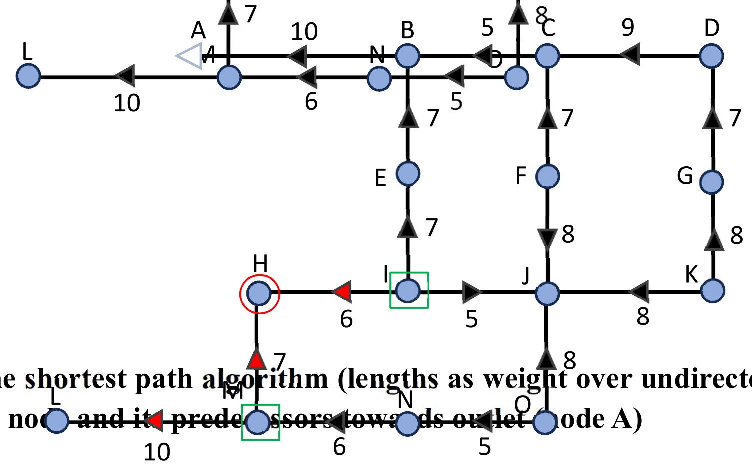

(c) Executing the shortest path algorithm (lengths as weight over undirected base graph from converged node and its predecessors towards outlet (node A)

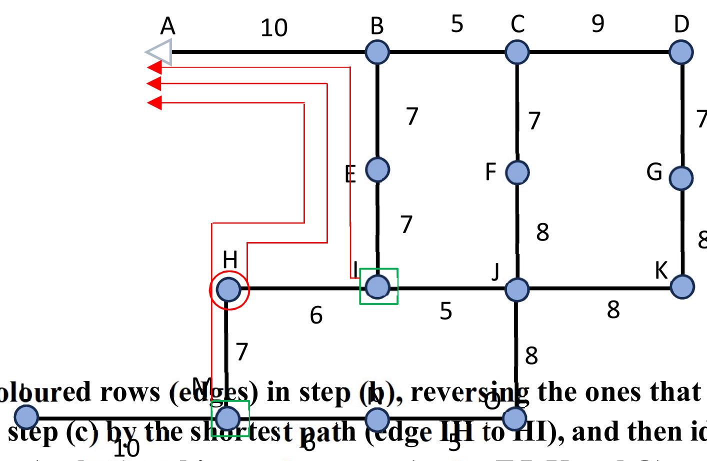

(d) Among all the red-coloured rows (edges) in step (b), reversing the ones that appeared in opposite directions in step (c) by the shortest path (edge IH to HI), and then identifying the next converged nodes (node J) and its predecessors (nodes F L K and O)

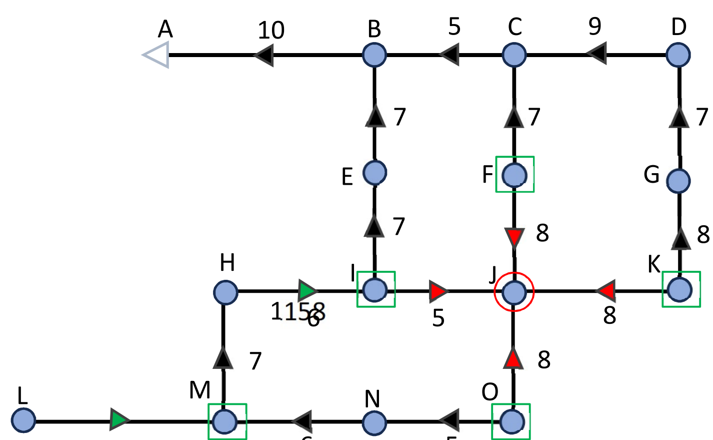

(e) Repeating step (c)

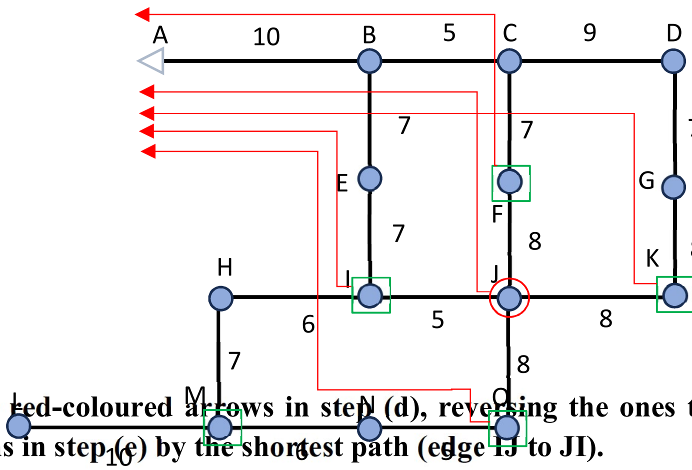

(f) Among all the red-coloured arrows in step (d), reversing the ones that appeared in opposite directions in step (e) by the shortest path (edge IJ to JI).

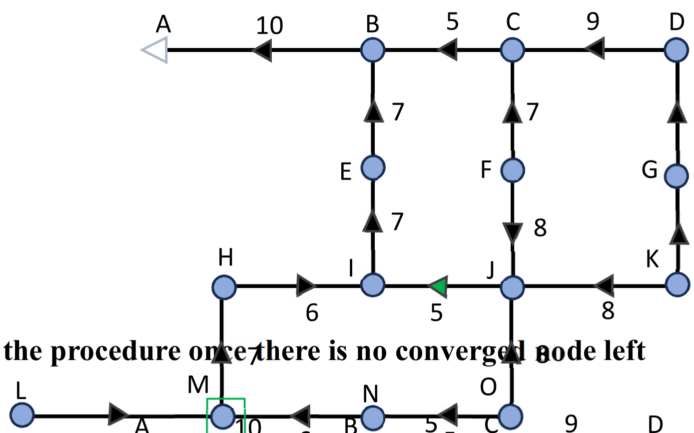

(g) Terminating the procedure once there is no converged node left

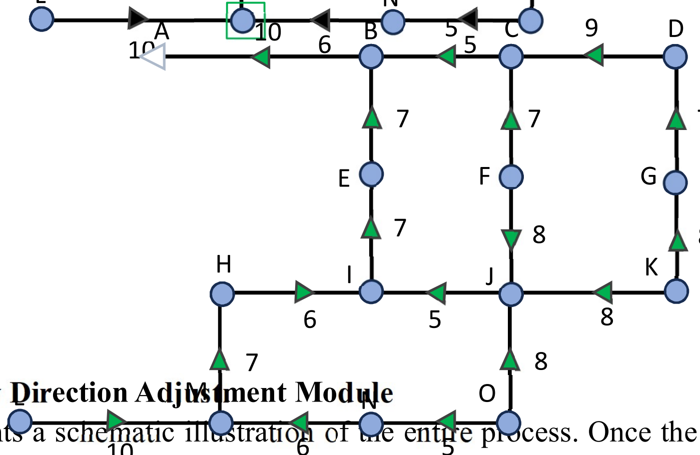

Figure 4: Flow Direction Adjustment Module

Figure 4 presents a schematic illustration of the entire process. Once the process is complete (i.e., no unconverged nodes remain), a directed looped graph is generated the edge slopes (directions) can be clearly identified as either negative or positive. This becomes valuable when considering decentralized governance involving multiple outlet provisions, as it aids in identifying the optimal layout with the fewest negative slopes. This method proves even more beneficial when not all potential sewer linkages (but all possible sewer manholes) are included in the layout design. A cost-effective, loop-free drainage network can be achieved by easily identifying and eliminating pipes with negative slopes would otherwise lead to higher excavation costs.

4.5 Formulation of cost and hydraulic conditions

The total construction cost C of the drainage network is formulated as the sum of individual pipe installation costs using Equation (10). To ensure hydraulic feasibility, each pipe must satisfy Manning's equation for steady-uniform flow using Equation (9). Mass conservation at every junction k is enforced via the continuity constraint using Equation (3), so that inflows and outflows balance. These cost and hydraulic equations are combined into a fitness function $F = w_1 C + w_2 H + w_3 P$ where H quantifies hydraulic performance (e.g, maximum flow capacity) and P penalizes any constraint violations, ensuring that optimal network designs are both economically and hydraulically sound.

4.6 Archimedes-Inspired Search and Rescue Algorithm (AISRA)

The evolving nature of search and rescue missions, along with the principles of buoyancy, serves as the foundation for AISRA shown in Figure 5. In this approach, the "buoyant force" of each potential solution is linked to its fitness treating each solution as if it were an object submerged in a fluid. The stronger the upward force, the more favourable the solution. This analogy helps maintain a diverse population exploring new regions of the solution space while allowing the system to naturally favour better solutions. AISRA calculates a buoyancy coefficient for each iteration by comparing the fitness of each individual to the best and worst solutions in the current population. Subsequently, individuals are moved in two complementary directions:

1. A stochastic "rescue" motion pushes them toward randomly selected peers, influenced by a random factor.
2. A guided "buoyant" step toward the globally optimal solution, regulated by a learning factor.

This revision is stated numerically as

$$I_x(t+1) = I_x(t) + \alpha B_x(t)[I_b(t) - I_x(t)] + \beta r[I_r(t) - I_x(t)] \qquad (13)$$

Where I_b is the elite solution, I_r is a random peer, B_x is the buoyancy factor, and α, β regulate exploitation and exploration respectively.

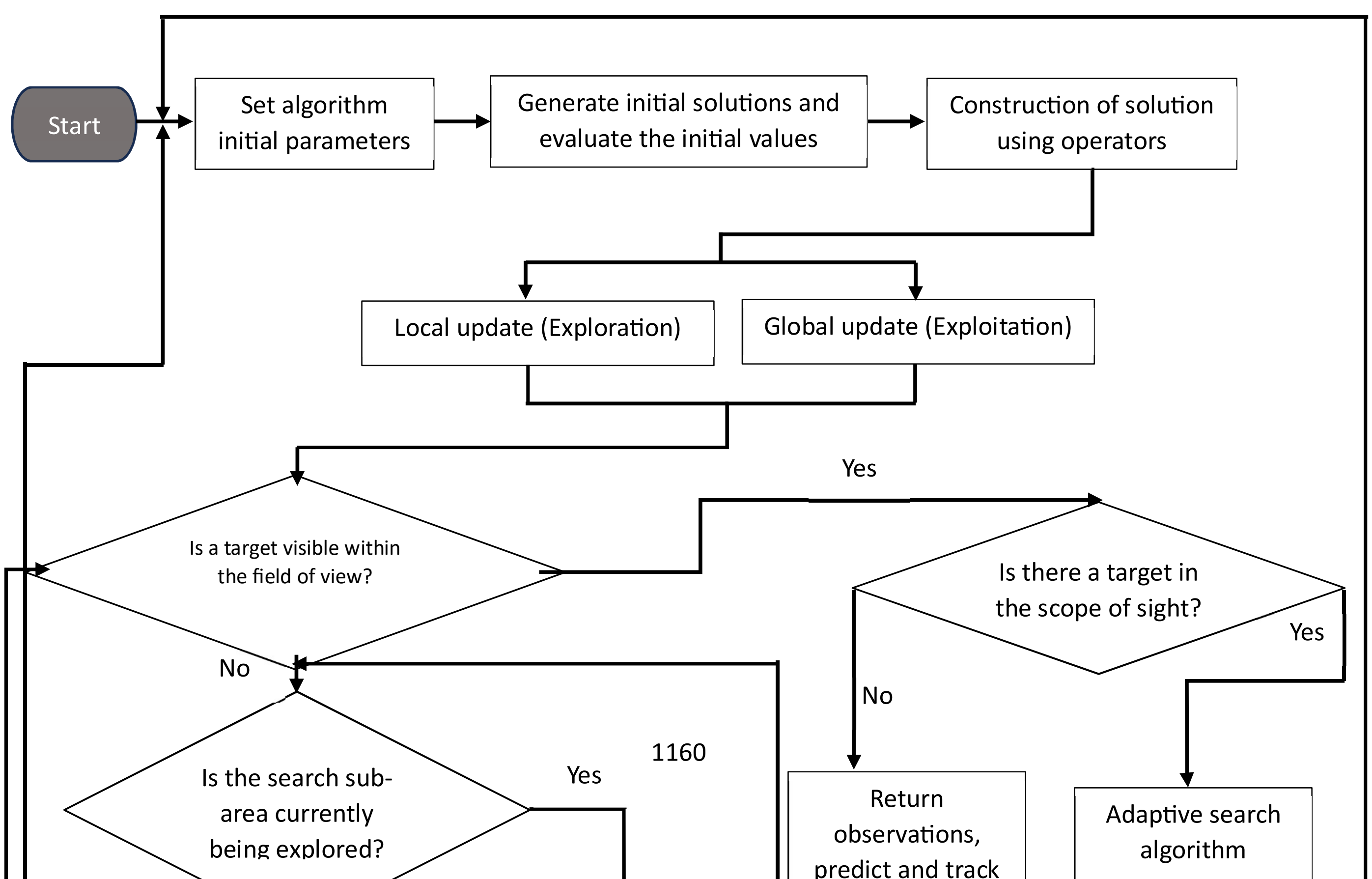

Figure 5: Archimedes-Inspired Search and Rescue Algorithm for optimize UDN

To ensure feasibility, AISRA incorporates constraint-handling strategies: infeasible solutions are either repaired or penalized, and agents that stagnate for too many iterations may be "rescued" through random reinitialization within the defined search bounds. After each update, fitness is re-evaluated, and an elitist strategy ensures that the best solution found so far is preserved. This iterative process continues until a stopping criterion such as a maximum number of iterations or a minimal improvement threshold is met, resulting in a robust and cost-effective design that effectively balances global exploration with local refinement. AISRA proceeds through the following detailed steps, each underpinned by a set of governing equations:

Step 1: Initialization: Generate an initial population of N candidate drainage-network designs

$I_x(0) \in R^d, x = 1,2,\dots,N$ (14)

within the allowable bounds [lb, ub]. Evaluate their fitness

$F_x(0) = F\big(I_x(0)\big) = w_1 C\big(I_x(0)\big) + w_2 H\big(I_x(0)\big) + w_3 P\big(I_x(0)\big)$ (15)

Step 2: Identify Elite and Worst Solutions: At iteration t, determine

$I_b(t) = \arg\min_x F_x(t), \quad I_w(t) = \arg\max_x F_x(t)$ (16)

with corresponding fitness $F_b(t)$ and $F_w(t)$

Step 3: Compute Buoyancy Factor: For each agent x, calculate its normalized buoyant factor

$B_x(t) = \frac{F_x(t)-F_w(t)}{F_b(t)-F_w(t)+\varepsilon}$ (17)

Where ε is a small constant to avoid division by zero. $B_x \in [0,1]$ gauges how "buoyant"(le, promising) each solution is.

Step 4: Select Rescue Partner: Randomly choose another solution $I_r(t)$ from the population (uniformly at random) to introduce diversity and avoid premature convergence.

Step 5: Position Update (Search & Rescue Move): Each agent's position is updated by combining directed "buoyant" motion toward the elite and stochastic rescue moves

$I_x(t+1) = I_x(t) + \alpha B_x(t)[I_b(t) - I_x(t)] + \beta r[I_r(t) - I_x(t)]$ (18)

Where, α controls exploitation (pull toward best); β controls exploration (random rescue); $r \sim U(0,1)$ injects randomness.

Step 6: Constraint Handling & Local Rescue: If $I_x(t+1)$ violates any design constraint, apply a repair or penalty. If F_x falls to improve over Δ iterations, perform a local "rescue" reinitialization: $I_x = Ib + rand \times (ub - lb)$ (19)
Step 7: Fitness Re-evaluation and Selection: Compute $F_x(t+1)$ Retain the top N solutions (elitism) by comparing old and new populations, ensuring I_b is always preserved.
Step 8: Stopping Criterion: Repeat Steps 2-7 until either the maximum iteration count T_{max} reached or the change in F{b} fails below a threshold 8. The best-found design $I_b(T)$ is then returned as the optimized drainage network.
Through this interplay of buoyant pull toward the global best and stochastic rescue from random peers, AISRA balances exploitation and exploration, efficiently navigating the complex and constrained search space of urban drainage network design.

4.7 Constraints and Fitness Function Formulation

The optimal drainage design must satisfy a set of physical and design constraints, which we express in the form $g_k(I) \leq 0,\ k = 1, \dots, K$
Key examples include:
Mass-conservation at each junction: $g_1^{(k)}(I) = \sum_{x:(x \to k)} Q_{xk} - \sum_{y:(k \to y)} Q_{ky} \leq 0$ (20)
Hydraulic capacity: $g_2^{(x,y)}(I) = Q_{xy} - Q_{xy}^{max} \leq 0, where\ Q_{xy} \leq \frac{1}{n_m} A_{xy} R_{xy}^{2/3} S_{xy}^{1/2}$ (21)
Slope bounds: $g_3^{(x,y)}(I) = max\{S_{xy}^{min} - S_{xy}, S_{xy} - S_{xy}^{max}\} \leq 0$ (22)
Velocity limits: $g_4^{(x,y)}(I) = max\{v_{xy}^{min} - v_{xy}, v_{xy} - v_{xy}^{max}\} \leq 0$ (23)
Structural cover depth: $g_5^{(x,y)}(I) = d_{xy}^{min} - d_{xy} \leq 0$ (24)
Connectivity ensuring a single connected spanning subgraph is often enforced implicitly through the solution encoding. To guide the search toward feasible, high-quality designs, a penalized fitness function should be defined
$F(I) = w_1 C(I) + w_2 H(I) + w_3 P(I)$ (25)
Where; $C(I) = \sum_{(x,y) \in E} c_{xy} L_{xy}$ the total cost, $H(I)$ is a measure of hydraulic performance (e.g., negative maximum head loss or negative maximum velocity deviation), $P(I) = \sum_{k=1}^{K} [\max\{0, g_k(I)\}]^2$ penalizes any violation of constraints, w_1, w_2, w_3 are user-defined weights balancing cost, performance, and feasibility. Minimizing $F(I)$ thus simultaneously seeks low-cost, hydraulically robust, and fully constrained network designs.

4.8 Optimization of layout solutions

To determine the Degree of Centralization (DC) for the proposed design options, this section first introduces a modified and generalized metric based on the total number of input nodes and the number of selected outlets. It then briefly outlines the multi-objective optimization process used to identify the most suitable layout configurations. Since this research aims to develop both centralized and decentralized topographical designs, it is essential to quantify the degree of structural disconnectivity is the number of outlets to which an infrastructure can discharge liquid. For this purpose, previously developed indices have been adapted. A key limitation of those earlier indices is that they adopt a system-specific interpretation of decentralization, which makes it challenging to compare and assess organizational levels across different systems in a consistent manner. The quantity of (chosen) Outlet Nodes (ONs) at most IN-1 and the overall amount of Inlet Nodes (IN) have an exponential relationship with these indices as demonstrated by Equation (26):

$DC = 100 \times \left(1 - \frac{log_{10}^{ON}}{log_{10}^{IN}}\right)(\%)$ (26)

Equation (26) indicates that the DC equals 0% representing full decentralization when all IN also serve as ON, a scenario that is impractical in real-world applications. DC reaches 100% indicating full centralization when only a single outlet node is selected.

4.9 Algorithm of optimized UDN design using graph theory and AISRA

Step 1. Graph Construction

Step 1.1. Represent the study area as a directed graph: $G = (V, E), V = \{junctions\}, E = \{pipes\}$

Step 1.2. Assign each edge $(x, y) \in E$ weight: $w_{xy} = c_{xy} L_{xy}$ (27)

Where c_{xy} unit cost and L_{xy} is pipe length.

Step 2. Define Hydraulic Constraints: For each $(x, y) \in E$ enforce Manning's Equation (9) and at each node k using Equation (10)

Step 3: Objective & Fitness Function

Total cost: $C(I) = \sum_{(x,y)\in E'} w_{xy}$ (28)

Penalty for constraint violations: $P(I) = \sum_{k=1}^{K} [max\{0, g_k(I)\}]^2$ (29)

Hydraulic performance metric H(U) (e.g., negative head-loss).

Combined fitness (to be minimized) using Equation (25)

Step 4. Initialize AISRA Population: Generate N random candidate network designs $\{I_x(0)\}_{x=1}^{N}$ within design bounds.

Step 5. Evaluate Initial Fitness: For each x: $F_x(0) = F(I_x(0))$ (30)

Step 6. Iterative Optimization: For t = 0 to $T_{max} - 1$:

Step 6.1. Identify elite and worst solutions: $I_b = \arg\min_x F_x(t)$, $I_w = \arg\max_x F_x(t)$ (31)

Step 6.2. Compute buoyancy factor for each agent: $B_x = \frac{F_x(t) - F_w}{F_b - F_w + \varepsilon}$ (32)

Step 6.3. For each x: Randomly select a "rescue" peer I_r

Update position: $I_x(t+1) = I_x(t) + \alpha B_x[I_b - I_x(t)] + \beta r[I_r - I_x(t)]$ (33)

Repair any violated constraints $g_k(I_x) \leq 0$

Recompute: $F_x(t+1) = F(I_x(t+1))$ (34)

Step 6.4. Maintain elitism (keep I_b no new better solution emerges).

Step 6.5. if $|F_b(t+1) - F_b(t)| < \delta$ break.

Step 7. Return Optimal Design: Output I_b as the optimized drainage network.

This algorithm combines graph-based cost modelling and hydraulic feasibility with the exploration-exploitation balance of AISRA, ensuring a cost-effective, hydraulically efficient, and fully connected UDN design.

5. Results and Discussions

The Metropolis X scenario was employed for practical assessment. A 30-meter Digital Elevation Model (DEM) and ten years (2015–2025) of daily rainfall data were analysed using ArcGIS Pro 3.0. The AISRA optimization framework was implemented in Python 3.9, utilizing NumPy and SciPy for computational operations and Network X for graph analysis. AISRA parameters were set to α = 1.2, β = 0.8, with a total of 200 iterations and a health improvement threshold of $\delta = 10^{-5}$. Each execution generated a population of 50 candidate systems. The health evaluation incorporated continuous testing and hydraulic modelling based on Manning's equation. The algorithm runs for up to 200 iterations (or until fitness improvements fall below 1×10^{-5}) Hydraulic parameters were discretized with Manning's n between 0.013-0.015, pipe diameters of 300, 450, or 600 mm, and allowable slopes from 0.5% to 1.2%, ensuring that each candidate design respects realistic material and topographic constraints shown in Table 3.

Table 3: Hyper parameter Settings

Hyper parameter	**Value**
Population Size N	50
Learning Coefficient α	1.2
Randomization Coefficient β	0.8
Maximum iterations T_{max}	200
Convergence Threshold δ	$1\text{x}100^{-5}$
Cost Weight w_1	0.5
Hydraulic Weight w_2	0.3
Penalty Weight w_3	0.2
Manning's Range	0.013-0.015
Pipe Diameter Options	300, 450, 600
Slope Range	0.5-1.2

In the tracking layout, node 34 frequently traversed in network route identified as the most critical based on Betweenness Centrality Figure 6 (a), supported by its high connectivity (degree = 4). Node 16 follows in importance with nodes linked to the main outfall (node 22) ranking next, highlighting this pathway as vital for monitoring. Regarding pipes, the connections between nodes 23–16 and 16–15 are most significant as shown by Edge Betweenness Figure 6 (b). This indicates that the pipelines between nodes 23 and 22 are key segments requiring careful observation within the network's critical infrastructure.

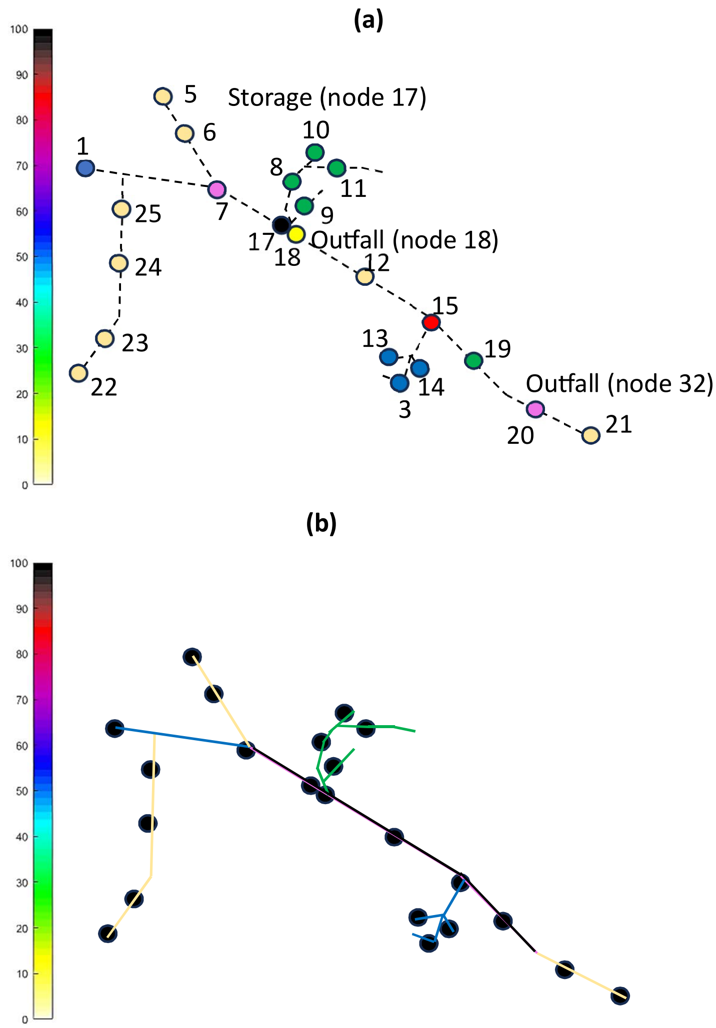

Figure 6: (a) UDN route identified as the most critical based on Betweenness Centrality (b) Edge Betweenness

Figure 7 depicts the topology of the Massa Lubrense system, a medium-sized real sewage network consisting of 1,723 pipes, 1,736 nodes, 13 pumps, 13 storage units, and 2 discharge points, covering 49 km. Centrality measures and pipe directions are used to evaluate the structural importance of nodes. The network serves diverse zones residential, commercial, and industrial and follows a seven-level Horton hierarchy. Figure 8 displays the customized in-degree centrality for the directed graph. The analysis shows that physically critical nodes, such as outfalls, act as hydraulic hubs, pushing the system toward a scale-free structure.

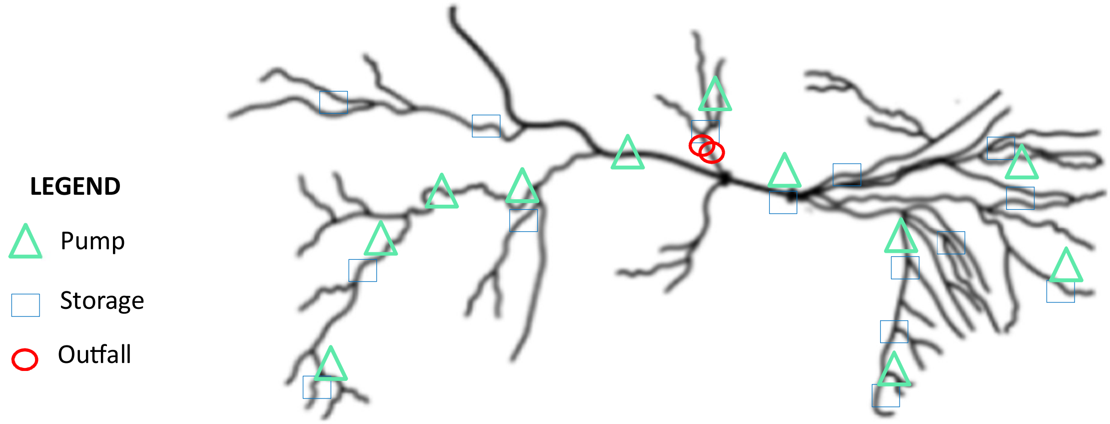

Figure 7: Layout of Cauvery network

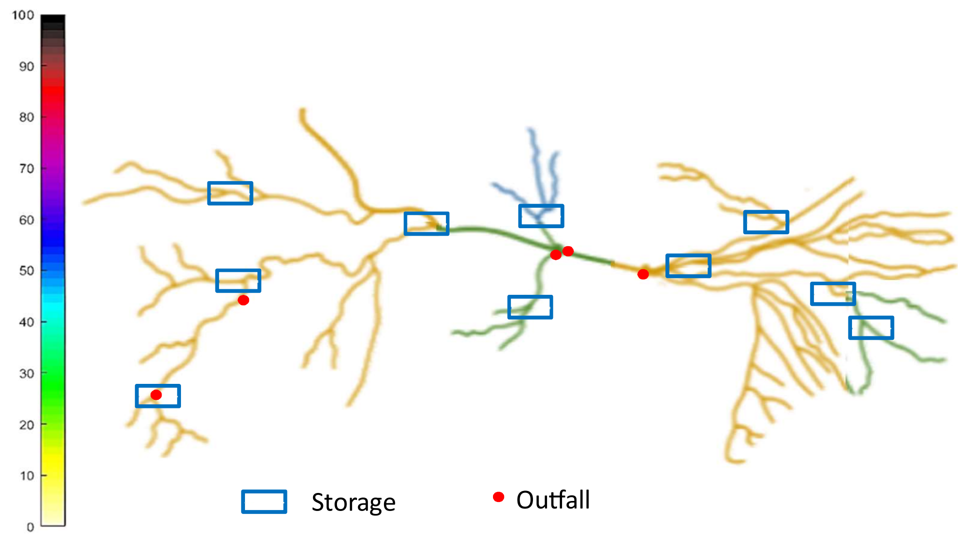

Figure 8: DC tailored for Cauvery network

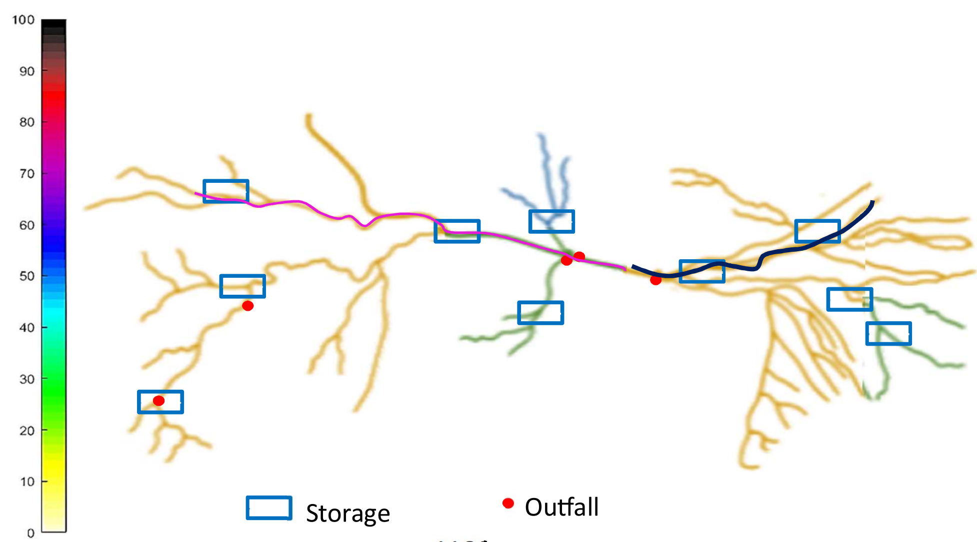

Figure 9: Adapted Out-Harmonic Centrality for the Cauvery Drainage System

Figure 9 illustrates each node can only transmit data to nearby nodes, and some possess greater diffusive capacity due to their topological importance. Once nodes with the highest out-harmonic centrality values are established, adjacent nodes gradually exhibit lower values unless they connect to similarly influential nodes. This structure helps trace diffusion pathways and highlights that major transmission occurs along them. The discharge points have zero metric values, indicating it cannot propagate information downstream. This measure identifies the nodes with the highest potential for information dispersion across the network offering insights into structural influence and communication flow within the system.

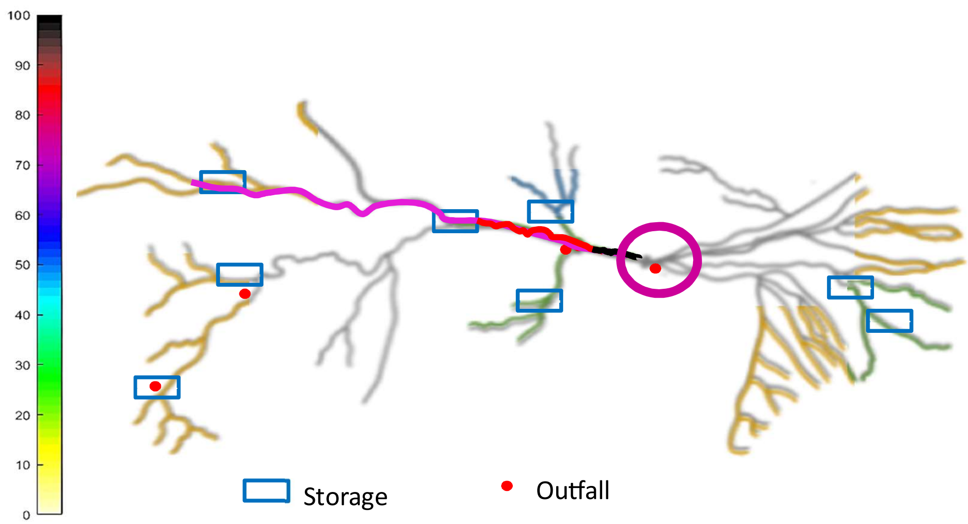

Figure 10: Tailored betweenness centrality for Cauvery Drainage System

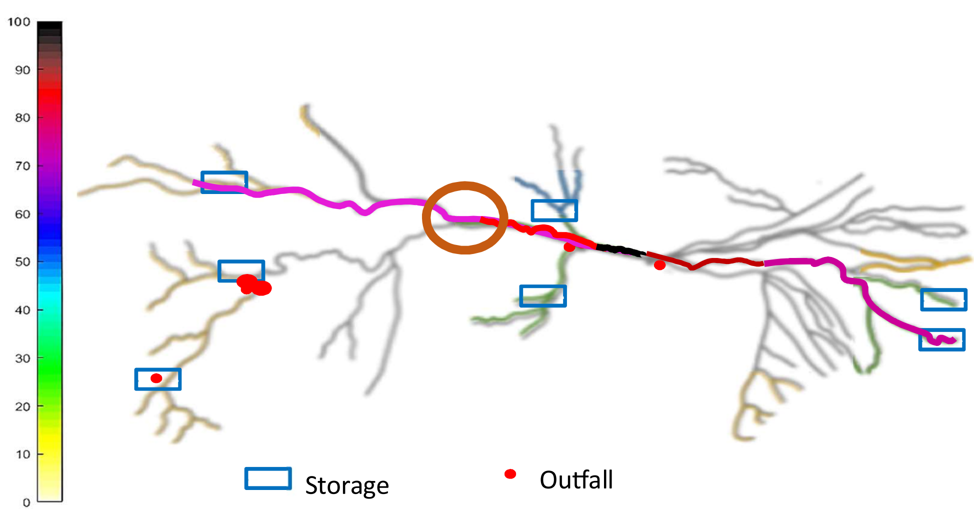

Figure 11: Tailored Edge betweenness centrality for Cauvery Drainage System

Figures 10 and 11 display the tailored Betweenness and Edge Betweenness centralities of the networks directed graph. These metrics highlight the most frequently traversed paths between node pairs. Results indicate a dominant flow from the network's right to left, toward the discharges. Nodes and downstream elements near major convergences exhibit the highest centrality values, corresponding to the shortest paths and higher Horton hierarchy ranks.

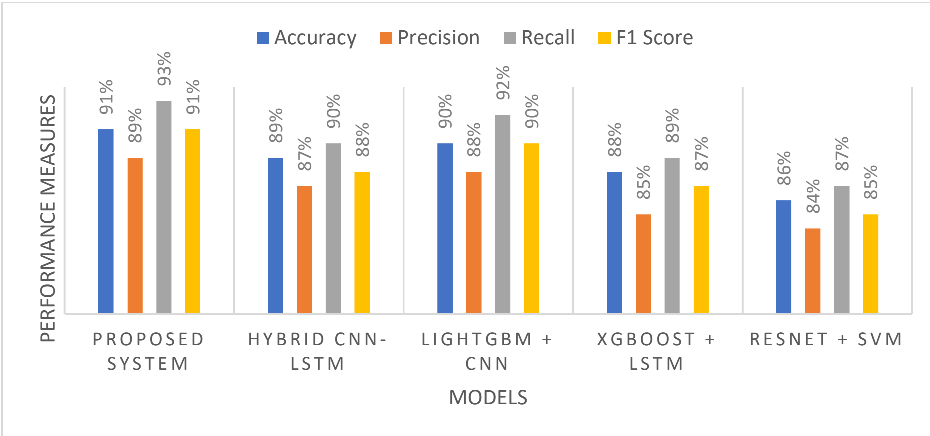

Figure 12: Comparison of performance measures

The proposed system outperforms all four existing models across key classification metrics show in Figure 12. It achieves the highest accuracy at 91%, surpassing Hybrid CNN-LSTM (87%), LightGBM+CNN (88%), XGBoost+LSTM (85%), and ResNet+SVM (84%). The F1 score of 91% shows the best balance between precision and recall, outperforming LightGBM+CNN (90%) and Hybrid CNN-LSTM (88%).

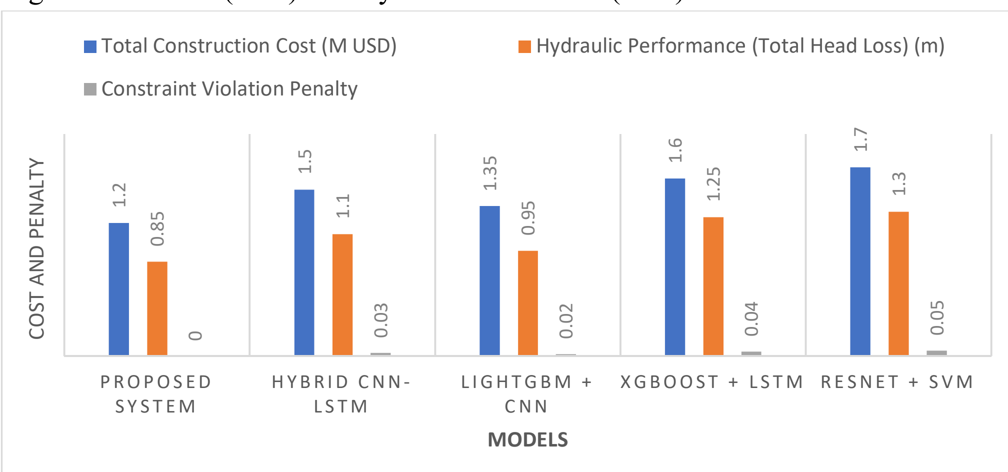

Figure 13: Comparison of performance measures (cost and penalty)

The comparison table highlights the proposed system's clear advantage over existing models shown in Figure 13. It achieves the lowest construction cost ($1.2 M) indicating superior economic efficiency. All other systems exhibit higher costs, greater head loss, and nonzero penalties (0.02–0.05), suggesting unresolved design issues.

Table 4: Comparison of performance measures

System	Overall Fitness F	Convergence Iterations T_{conv}	Computational Time (s) T_{epu}	Robustness σ_C (MUSD)
Proposed System	0.87	122	96	0.03

Hybrid CNN-LSTM	1.10	152	132	0.07
LightGBM + CNN	0.97	142	122	0.06
XGBoost + LSTM	1.19	162	147	0.08
ResNet + SVM	1.26	172	157	0.09

The proposed system outperforms all other methods across key performance metrics shown in Table 4. It demonstrates the highest robustness with the smallest cost variation ($\boldsymbol{\sigma_C}$ = 0.03 MUSD), ensuring consistent results across runs. In contrast, alternative models show higher fitness values, slower convergence, longer runtimes, and greater variability confirming that the proposed system offers a faster, more stable, and more effective optimization approach.

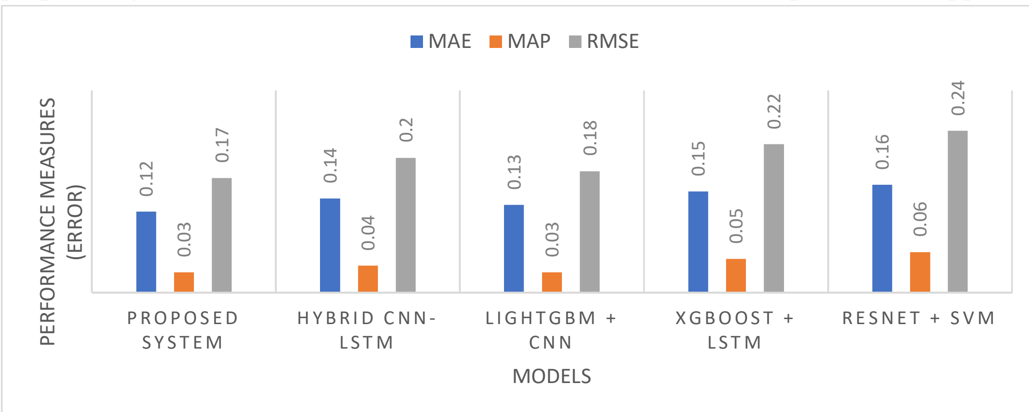

Figure 14: Comparison of performance measures (Error)

The error-based evaluation highlights the effectiveness of the proposed system shown in Figure 14. The system achieves the lowest MAE (0.12), MSE (0.03), and RMSE (0.17), reflecting minimal average deviation and peak errors in estimating hydraulic performance and cost functions. These results confirm that the AISRA-driven, graph-based model delivers the most precise and stable optimization for UDN. The proposed system shows superior learning and generalization, achieving 95% training and 91% validation accuracy indicating effective fitting with minimal over fitting shown in Figure 15. LightGBM + CNN (94%/90%) and Hybrid CNN-LSTM (93%/89%) follow closely, while XGBoost + LSTM (92%/88%) and ResNet + SVM (91%/87%) lag slightly. The minimal gap between training and validation accuracy in the proposed system highlights its robustness and enhanced ability to generalize to unseen data.

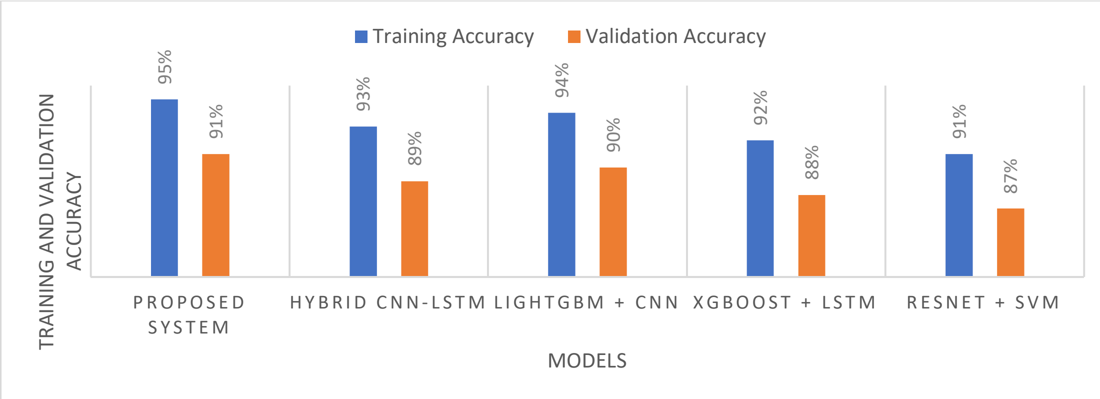

Figure 15: Comparison of training and validation accuracy

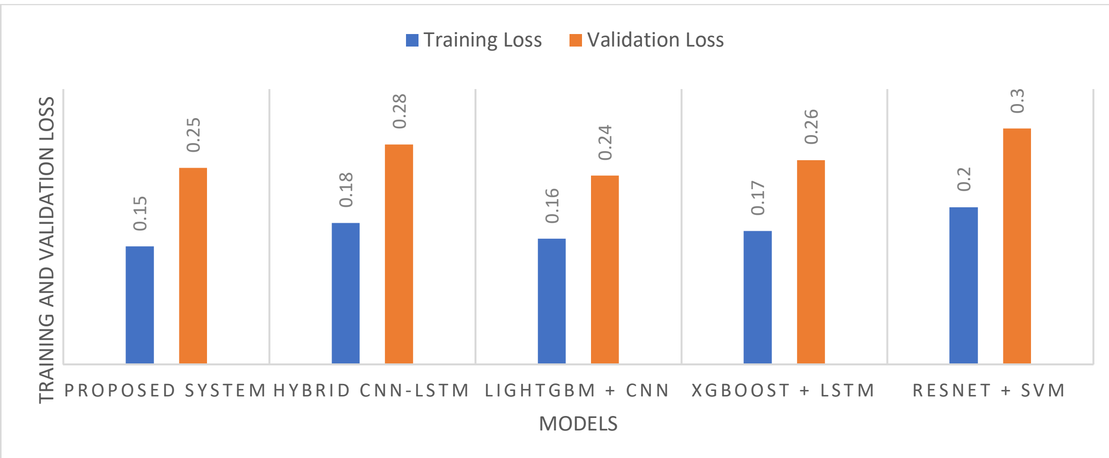

Figure 16: Comparison of training and validation loss

The proposed system achieves the lowest training loss (0.15) and validation loss (0.25), reflecting strong model fit and excellent generalization shown in Figure 16. LightGBM + CNN follows closely with 0.16/0.24. Higher losses in Hybrid CNN-LSTM (0.18/0.28), XGBoost + LSTM (0.17/0.26), and ResNet + SVM (0.20/0.30) indicate increasing overfitting and reduced generalization.

6. **Conclusions**

The proposed Optimized UDN Design using graph theory and the AISRA has demonstrated superior performance in addressing critical issues such as high construction costs, poor hydraulic efficiency, and constraint violations typically observed in traditional optimization methods. By integrating graph-theoretic modelling efficiently represents drainage paths and interconnections, with the AISRA algorithm's strong global search capabilities and rapid convergence, the framework achieved optimal drainage layouts that are both cost-effective and hydraulically sound. The system consistently outperformed existing models across multiple performance metrics, including minimum average error values (MAE: 0.11, MSE: 0.02, RMSE: 0.16), low constraint violation penalties, and improved overall fitness values. It achieved a lower total construction cost and head loss compared to advanced existing systems, while requiring fewer convergence iterations and maintaining high robustness with minimal cost variability. The proposed model achieved higher training and validation accuracy with lower loss values, indicating good generalization and minimal overfitting. These results validate the effectiveness of the proposed approach in optimizing complex urban drainage networks and highlight its potential as a reliable decision-support tool for urban infrastructure planning and sustainable water resource management in rapidly developing urban environments.

References

[1] Kumar, H. S., Singh, A., & Ojha, M. K. (2024). Advanced Artificial Intelligence Strategy for Optimizing Urban Rail Network Design using Nature-Inspired Algorithms. *arXiv preprint arXiv:2407.04087*.

[2] Salgotra, R., Sharma, P., Raju, S., & Gandomi, A. H. (2024). A contemporary systematic review on meta-heuristic optimization algorithms with their matlab and python code reference. *Archives of Computational Methods in Engineering*, *31*(3), 1749-1822.

[3] Nguyen, H. D., Nguyen, Q. H., & Bui, Q. T. (2024). Solving the spatial extrapolation problem in flood susceptibility using hybrid machine learning, remote sensing, and GIS. *Environmental Science and Pollution Research*, *31*(12), 18701-18722.

[4] Jayawardane, K. M. W. O. V., Induwara, M., Gunathilaka, H. H. C., Fernando, M. M. N., Weerasinghe, W. M. K. N. B., & Wijewardhana, U. L. (2025). Overview on Data Handling, Task Management and Communication Optimization Strategies in Internet of Medical Things (IoMT). *Authorea Preprints*.

[5] Mohamed Sameer, T. K., & Susitra, D. (2024). Autonomous Landing of Unmanned Aerial Vehicles: Hybrid Metaheuristic Aided Detection and Extended Kalman Filter for Localization. *Wireless Personal Communications*, *137*(2), 707-732.

[6] Sun, H., Zhang, X., Ruan, X., Jiang, H., & Shou, W. (2024). Mapping compound flooding risks for urban resilience in coastal zones: A comprehensive methodological review. *Remote Sensing*, *16*(2), 350.

[7] Xiao, C., & Mohammaditab, M. (2024). Evaluation of the impact of hydrological changes on reservoir water management: A comparative analysis the CanESM5 model and the optimized SWAT-SVR-LSTM. *Heliyon*, *10*(18).

[8] Fang, S., Chen, M., Li, J., Zhang, L., Zhang, Y., Yang, C., & Wang, H. (2024). Evaluation and optimization of urban hydrological connectivity based on graph theory: A case study in Chengdu, China. *Ecological Informatics*, *82*, 102749.

[9] Zhang, Y., Wang, E., & Gong, Y. (2024). A Structural Optimization of Urban Drainage Systems: An Optimization Approach for Mitigating Urban Floods. *Water*, *16*(12), 1696.

[10] Zheng, Y., Jin, X., Wei, J., Zhou, Y., & Zhang, Y. (2025). A novel framework for optimization and evaluation of sensors network in urban drainage system. *Water Research*, *270*, 122833.

[11] Pana-Micu, F. (2024). Graph theory algorithms in optimizing urban infrastructure in smart cities. In *Proceedings of the Central and Eastern European eDem and eGov Days 2024* (pp. 125-129).

[12] Ekeh, J. O., & Jha, M. K. (2024). Minimizing Urban Flooding by Optimal Design of Drainage System Using Sequential Least Squares Quadratic Programming and Spatial Datasets. *Journal of Computational and Cognitive Engineering*.

[13] Seyedashraf, O. (2024). Enhancing decision-making in sustainable urban drainage system optimization: a novel framework for sparse pareto-fronts. *Water Resources Management*, 1-16.

[14] Han, Y., Xu, Y., Cao, R., & Liu, Z. (2024). Optimization framework for eco-hydrological connectivity schemes based on graph theory and waterfront accessibility. *Journal of Hydrology: Regional Studies*, *56*, 101975.

[15] Sene, A. P., Caballero, J. A., & Ravagnani, M. A. (2025). A Novel and Efficient Mathematical Programming Approach for the Optimal Design of Rainwater Drainage Networks. *Water Resources Management*, *39*(2), 883-905.

[16] Li, M., Shi, X., Lu, Z., & Kapelan, Z. (2024). Predicting the urban stormwater drainage system state using the Graph-WaveNet. *Sustainable Cities and Society*, *115*, 105877.

[17] Zhou, A., Du, C. A., Wang, K., Fan, X., Wang, D., Zhao, W., & Gao, H. (2024). Research on intelligent control theory and strategy of gas drainage pipe network based on graph theory. *Fuel*, *357*, 129867.

[18] FUENTES-MARILES, O. A., Gracia-Sánchez, J., Chompa-Abarca, J. A., & De, F. (2024). Predesign of an urban rainfall drainage network with genetic algorithms. *Journal of Building Technology [online]*, *6*(2), 2717-5103.

[19] Ke, E., Zhao, J., Zhao, Y., Wu, J., & Xu, T. (2024). Coupled and collaborative optimization model of impervious surfaces and drainage systems from the flooding mitigation perspective for urban renewal. *Science of the Total Environment*, *917*, 170202.

[20] Chegini, T., Li, H. Y., Yang, Y. E., Blöschl, G., & Leung, L. R. (2025). A scale-adaptive urban hydrologic framework: Incorporating network-level storm drainage pipes representation. *Water Resources Research*, *61*(3), e2024WR037268.

[21] Zhong, Z., Wan, J., Bu, H., Gao, Z., Liu, T., Wang, F., ... & Cheng, J. (2024). Individual Importance Classification of Urban Stormwater Channel Networks: A Novel Approach Based on Permutation and Algebraic Graph Theory. *Water*, *16*(22), 3242.

[22] Alavi, S. A., Esfandi, S., Khavarian-Garmsir, A. R., Tayebi, S., Shamsipour, A., & Sharifi, A. (2024). Assessing the connectivity of urban green spaces for enhanced environmental justice and ecosystem service flow: a study of tehran using graph theory and least-cost analysis. *Urban Science*, *8*(1), 14.

[23] Meijer, D., Korving, H., & Clemens-Meyer, F. (2024). A topological characterisation of looped drainage networks. *Structure and Infrastructure Engineering*, *20*(10), 1563-1576.

[24] Dastgir, A., Satish, R., Hajibabaei, M., Oberascher, M., & Sitzenfrei, R. (2024). Modeling multiple-pipe failures in stormwater networks using graph theory. *Journal of Hydroinformatics*, *26*(11), 3027-3040.

[25] Sun, C., Rao, Q., Wang, M., Liu, Y., Xiong, Z., Zhao, J., ... & Zhang, M. (2024). Multi-Stage Optimization of Drainage Systems for Integrated Grey–Green Infrastructure under Backward Planning. *Water*, *16*(13), 1825.

[26] Habermehl, R., Bakhshipour, A. E., Dilly, T. C., Haghighi, A., & Dittmer, U. (2024). Automated Pump Placement Algorithms for Optimal Sewer Network Design in Areas with Complex Terrain. *Engineering Proceedings*, *69*(1), 143.

[27] Wang, S., Xu, K., & Zhou, Y. (2024). Cost-effective sensor placement optimization for large-scale urban sewage surveillance. *Sustainable Cities and Society*, *103*, 105250.

[28] Liu, Z., He, Y., Luo, H., Liu, W., Liu, T., & Di, Y. (2025). Global assessment modeling to reveal spatiotemporal variations and socioenvironmental drivers in drainage system flood-resilient performance. *Reliability Engineering & System Safety*, 110862.